GEOLOGY | THE GEOLOGICAL SOCIETY OF AMERICA®

https://doi.org/10.1130/G52408.1

Manuscript received 24 May 2024
Revised manuscript received 7 October 2024
Manuscript accepted 25 October 2024

Published online 20 November 2024

On the relationship between the uppermost mantle (≤220 km) seismic velocity, crustal thickness, and topography in Tibet

David B. Rowley[1,*], Chujie Liu[2,4], Stephen P. Grand[2], Xiaofeng Liang[3], and Eric Sandvol[4,†]

[1]Department of the Geophysical Sciences, University of Chicago, Chicago, Illinois 60637, USA
[2]Department of Geological Sciences, University of Texas at Austin, Austin, Texas 78712, USA
[3]State Key Laboratory of Lithospheric and Environmental Coevolution, Institute of Geology and Geophysics, Chinese Academy of Sciences, Beijing 100029, China
[4]Department of Geological Sciences, University of Missouri, Columbia, Missouri 65211, USA

ABSTRACT

We propose that the mantle lithospheric density and crustal thickness are correlated in such a way as to produce a flat Tibetan Plateau. We observe that the mantle lithosphere is relatively uniform beneath the Himalaya and southern and central Tibet, despite a near doubling of crustal thickness relative to India. Farther north, cratonic mantle lithosphere disappears over large regions of north-central Tibet, giving rise to large lateral variations in uppermost mantle Vs anomalies (>12%) that are uncorrelated with changes in surface elevation but are closely related to changes in crustal thickness. This decoupling of surface topography from spatial variations in upper mantle seismic velocity, and assumed buoyancy, implies that Tibetan topography is controlled by a crust-mantle interaction that is able to maintain its near constant elevation. This crust-mantle interaction is likely driven by gravitational potential energy with a very weak crust. Magmatism, with ages of ca. 20 Ma to Present, spatially correlated with this region with no sub-Moho mantle lithosphere implies destabilization of mantle lithosphere in northern Tibet. Cratonic Indian underthrusting for the past 25 m.y. has also not led to significant topography in the plateau through time. The magmatism may have helped weaken the crust, allowing it to respond to changes in uppermost mantle buoyancy, resulting in a flat plateau.

INTRODUCTION

The Tibetan Plateau and adjacent Himalaya are the largest area of high (>4 km) topography on Earth. The origin and evolution of that topography has been the subject of discussion and modeling since Argand (1924) first speculated that the high topography correlates with a doubling of the thickness of the continental crust due to underthrusting of Greater India. Airy isostatic models focus on the crustal contribution to the topography (Fig. 1A). England and Houseman (1986) and Molnar et al. (1993) introduced the current paradigmatic model emphasizing the role of lithospheric mantle to understanding the topography. In their model, convergence and associated distributed shortening and thickening affect both crust and mantle lithosphere (Fig. 1). Regions of increased crustal thickness control the distribution of topography, with the surface height increasing with crustal thickness. Countering this crustal isostatic elevation is a reduction of surface height with increasing lithospheric mantle thickness (Fig. 1). An important aspect of the Molnar et al. (1993) modeling was to point out that as a thickened mantle lithosphere became convectively destabilized and sank into the underlying mantle, the surface topography would increase significantly (up to 2 km) and rapidly. Thus, the inclusion of mantle lithosphere in this model framework allows for significant elevation changes with little or no changes in crustal thickness, thereby potentially decoupling paleo-elevation history from crustal deformation. Similar uncoupling has been suggested to result from lower to mid-crustal flow, best exemplified beneath regions of eastern Tibet (Royden, 1997).

Various attempts to test the Molnar et al. (1993) model have been applied with varying degrees of certainty. For example, Rowley and Currie (2006) used stable isotope paleoaltimetry from the Lunpola Basin in the center of the Tibetan Plateau to argue for little or no discernable change in paleo-elevations since the late Eocene. Alternatively, recent models of paleoaltimetry measurements suggest the presence of a longitudinal valley roughly corresponding to the Lhasa block prior to the beginning of the Miocene (Valdes et al., 2019; Ding et al., 2022). In the early Miocene, the Lhasa block likely experienced crustal weakening and thickening possibly caused by volcanism related to a slab breakoff event (Liang et al., 2023). This alternative model indicated that there has been very little change in plateau topography for the past 20 m.y.

In terms of the subsurface structure, seismic tomography has always been an important tool, although there has been a lack of agreement on the first order features of the Tibetan uppermost mantle from a variety of tomographic models using different approaches. Recently, a series of full waveform tomographic models have been published (Ma et al., 2022; Liu et al., 2024) that largely agree to first order on the nature of the uppermost mantle beneath the Tibetan Plateau (Dou et al., 2024).

Here, we utilize the new full waveform seismic tomographic method and model FWEA2023 (Tao et al., 2018; Liu et al., 2024) that allows an explicit test of the correlation among upper mantle seismic velocity anomalies, topography, and crustal thickness (Fig. 2A). Values of shear wave velocity anomaly (dVs) extracted from the model have a horizontal spacing of 0.25 arcdegrees and a depth spacing of 10 km. Here, we

Eric Sandvol https://orcid.org/0000-0002-3082-9149
*Deceased
†sandvole@missouri.edu

CITATION: Rowley, D.B., et al., 2025, On the relationship between the uppermost mantle (≤220 km) seismic velocity, crustal thickness, and topography in Tibet: Geology, v. 53, p. 166–170, https://doi.org/10.1130/G52408.1

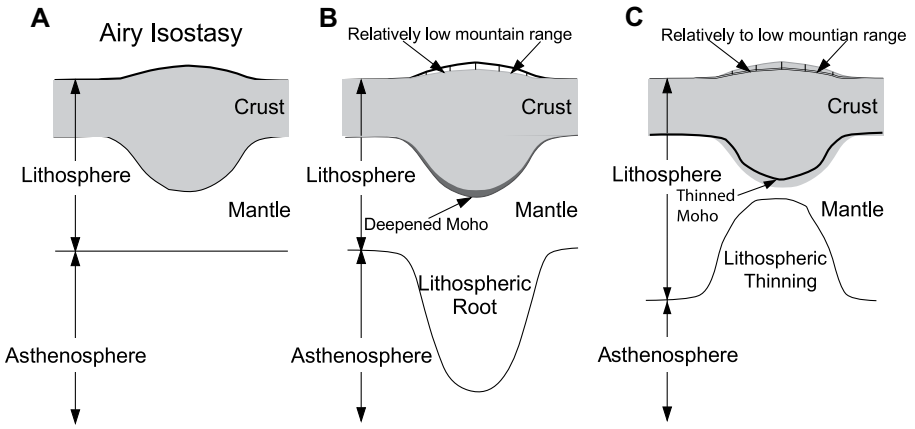

Figure 1. Simple conceptual models following Molnar et al. (1993). Thickened and thinned mantle lithosphere is associated with lowered topography (vertical line shading) and raised topography respectively (dark line).

focus on the better resolved shear wave velocity anomalies in the Tibet portion of the model.

RESULTS

The shear wave velocity anomaly in the uppermost mantle beneath the Tibetan Plateau crust varies from ∼−6% slow to >+12% fast relative to FWEA-18_REF (Tao et al., 2018). A significant fraction of the Tibetan Plateau is underlain by very fast (≥5%) upper mantle that is continuous to the south across the Himalaya with Indian cratonic mantle lithosphere (CML) (Figs. 2A, 2B, 3A, and 3B). This CML is relatively uniform in thickness, generally extending to depths shallower than 220 km (Fig. 3). The northern limit of what is inferred to be Indian CML (dVs ≥5%) is irregular, extending considerably farther north under eastern central Tibet, only to ∼31°N at 90°E (Fig. 2). In the west, where the Tarim Basin is adjacent to northern Tibet, CML underlying Tarim is juxtaposed with cratonic India, and here thicknesses are somewhat greater, but generally only by a few tens of km, despite the underlying crust being ∼80 km thick (Liang et al., 2023).

Immediately north of the edge of inferred Indian CML, much of the north central Tibetan Plateau is underlain by significantly slower (to −6%, mostly <0% to −3%) upper mantle from the Moho down to 210 km or deeper. In this region there is no lithospheric mantle separating the crust and asthenospheric mantle, as judged by dVs anomalies ≤0% below the Moho and above 220 km depth. The absence of lithospheric mantle accords with estimates of lower crustal temperatures ≥800 °C from crustal xenoliths in this area (Hacker et al., 2000). This region of slow velocity anomalies is bounded in the NW by the Altyn Tagh fault, and western and central Kunlun to the north (Fig. 2). The >10% difference in shear wave velocity anomaly over short distances (<200 km) (Figs. 2 and 3) and other models show a similar pattern (Schaeffer and Lebedev, 2013; Ma et al., 2022; Dou et al., 2024).

The region of slow shear wave velocity anomalies underlying north central Tibet is almost continuously underlain by faster mantle materials with anomalies generally in the range of ≥1% to +3% fast at depths typically between ∼80 km and ∼290 km (Fig. 3A), but locally to ∼500 km (Fig. 3B). Along many sections, some of this fast material is continuous with much faster CML materials at shallower depths either to the north or south. In some sections, larger blob-like structures of fast (typically >+1% to +3%) material are radially continuous over distances of up to 300 km (Fig. 3B), whereas in others they retain a more tabular appearance, with horizontal dimensions of mostly >200 km (Fig. 3A), but are themselves discontinuous in three dimensions as demonstrated by the contrasts of Figures 3A and 3B.

INTERPRETATION

Underthrust Cratonic Mantle Lithosphere

The Indian CML that underlies the Himalaya and southern Tibetan Plateau appears largely undeformed; that is, it does not significantly thicken relative to CML south of the Himalaya, despite underlying crust that is approximately twice the normal crustal thickness. Thus, models incorporating concomitant shortening and thickening of the crust and mantle lithosphere (Fig. 1; England and Houseman, 1986; Molnar et al., 1993) and many more recent studies are not supported by these data. Rather simple progressive northward underthrusting of Indian CML beneath Himalayan and Tibetan crust appears to dominate the more recent (ca. <25 Ma) collisional history. The absence of significantly fast (>+5%) mantle deeper within the upper mantle beneath southern Tibet, the Himalaya, or northern India suggests that CML has generally been resistant to convective destabilization and sinking into the mantle (Liu et al., 2024).

Northern Tibet Slow Upper Mantle

A critical component of models derived from England and Houseman (1986) and Molnar et al. (1993) is the emphasis on the impact on surface topography of the replacement of convectively destabilized denser mantle lithosphere by less dense, hotter, upwelling asthenospheric mantle. In their conceptual model, this exchange is tied to an increase in height of the topographic surface, and in the elegant synthesis of Molnar et al. (1993), this increased height is argued to correlate with associated transformations of the broader India-Asia collisional system: onset of E-W extension across the Himalaya and Tibetan Plateau, onset of deformation of the Indian oceanic lithosphere to the south, and onset of the Indian monsoon and coastal upwelling off east Africa, among others.

The cross sections (Fig. 3) show no discernable variation in surface height despite significant lateral variation in upper mantle shear wave anomalies between the Moho and 220 km. The presence of deeper significantly fast (>1%) velocity anomalies below this region (Fig. 3) is compatible with convectively destabilized denser lithospheric materials sinking in the upper mantle, and thus with our inferences regarding relative densities. The presence of radially elongated volumes of seismically fast material under parts of this region (Fig. 3B) that we interpret as Raleigh-Taylor–like drips, is also compatible with this inference. In addition, there is a clear spatial correlation between the distribution of 20 Ma and younger mantle-derived magmatism (Chapman and Kapp, 2017; Hacker et al., 2000) with slow uppermost mantle (≤220 km) dVs anomalies (Fig. 2B) and lower crustal temperatures inferred from xenoliths (Hacker et al., 2000) associated with the replacement of lithospheric mantle with asthenosphere immediately below the crust (Fig. 3). The spatial correlation of magmatism with absence of mantle lithosphere below the crust implies destabilization by ca. 20 Ma in this region.

Crustal Control on Mean Plateau Elevation

We have explored the correlation between crustal thickness and uppermost mantle Vs structure of the upper 220 km. We have used the crustal thickness model of Liang et al. (2023) and the crustal density model of Hao et al. (2023) to estimate the uppermost mantle density necessary to maintain 5 km of topography, given that the plateau is in isostatic equilibrium (e.g., McKenzie et al., 2019). The result of our analysis is shown in Figure 4A, and we see a very similar picture as is shown in Figure 2B, where low Vs values correlate nearly perfectly with the estimated low-density anomalies required to support the topography across the entire plateau. It is important to emphasize that we have not used any of the Liu et al. (2024) model to generate Figure 4A. Furthermore, Figure 4B explicitly examines this correlation by comparing Tibetan Plateau

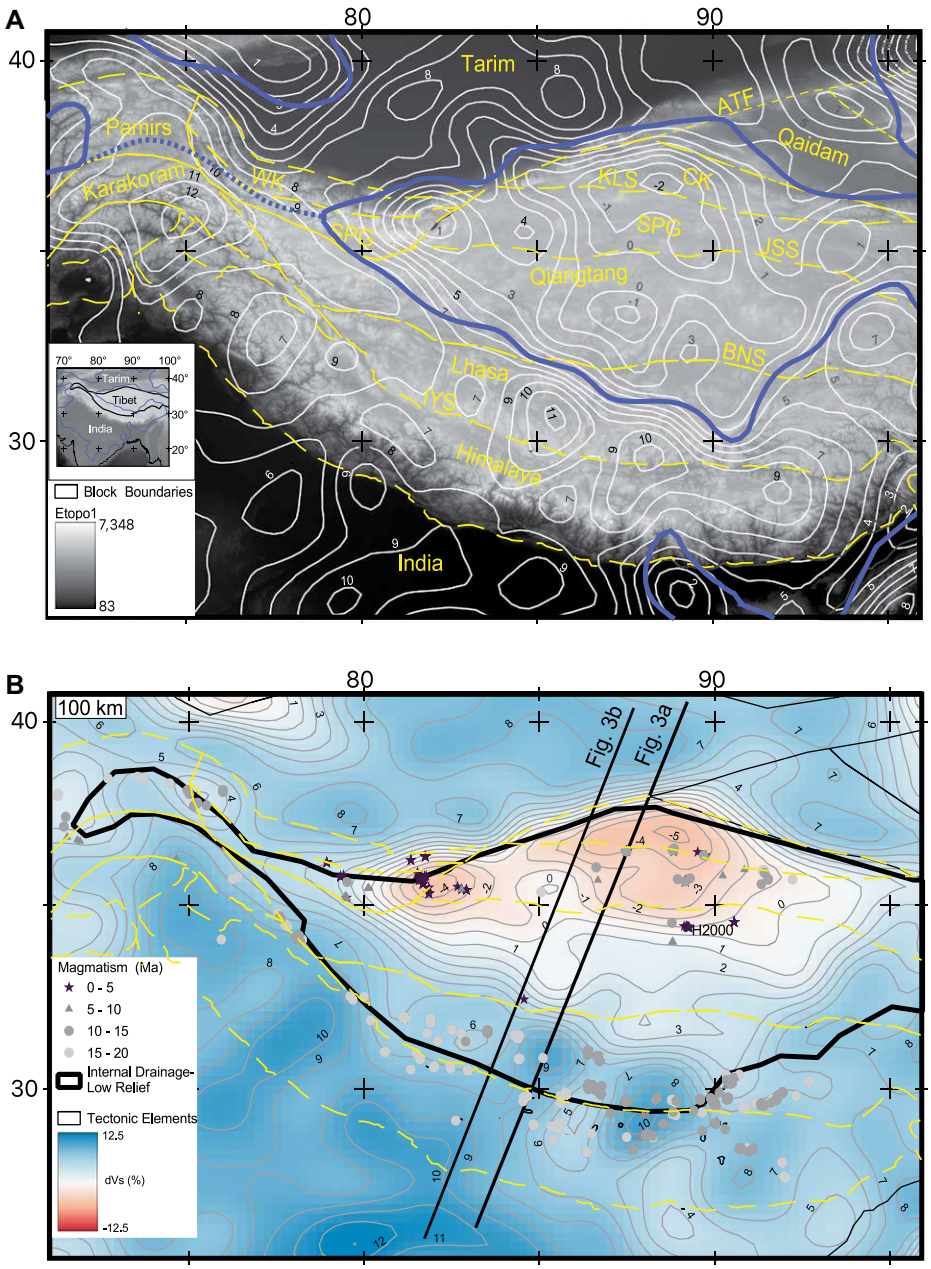

Figure 2. (A) Present topography of the Himalaya and Tibet region (Amante and Eakins, 2009). Shear wave anomaly contours are shown in white at 150 km depth. Dashed yellow lines are simplified tectonic block boundaries from Parsons et al. (2020). The black line outlines the region of mostly internal drainage and an elevation above 3500 m. Blue line is the 5% contour at 100 km depth outlining Indian, Tarim, and Qaidam cratonic lithosphere mantle. ATF—Altyn Tagh fault; BNS—Banggong Co-Nujiang suture; CK—central Kunlun; IYS—Indus-Yarlung suture; JSS—Jinsha suture; KLS—Kunlun suture; SPG—Songpan-Ganze; WK—western Kunlun. (B) Shear wave anomaly map at 100 km depth with 1% contours, and locations of magmatism in 5 Ma intervals from Chapman and Kapp (2017). Locations of cross sections in Figure 3. H2000 marks the xenolith locality of Hacker et al. (2000).

elevations and shear wave anomaly at a depth of 150 km (Fig. 2A). There is no correlation of present-day topography and upper mantle seismic velocity across the low-relief, primarily internally drained portions of the Tibetan Plateau. The clear implication is that the height of the Tibetan Plateau is not correlated with upper mantle seismic velocity structure.

Since crustal thickness correlates nearly perfectly with changes in uppermost mantle density, we believe this further confirms the inference that shear wave velocity anomalies are representative of density anomalies. This returns the problem to its historical roots (Argand, 1924). The observation from Figures 4A and 2B that juxtaposition of fast and presumably negatively buoyant mantle with slow, positively buoyant asthenospheric upper mantle beneath much of north central Tibet does not impact surface topography implies that crustal thickness adjusts itself to mantle density changes to maintain flat topography and isostasy. It is worth noting that it is possible there were some transient topographic highs or lows although present-day Tibet is quite flat (Fig. 1). Crustal adjustments can be reasonably modeled in terms of the Argand number (England and McKenzie, 1982) that effectively sets a limit on the crustal thickness and hence mean elevation of the plateau region. We envision that perturbations to the base of the crust due to uppermost mantle anomalies generate gradients in the gravitational potential energy that generates crustal flow similar to that described in McKenzie et al. (2019). Lower to mid-crustal flow thereby isolates surface topography from the underlying mantle buoyancy distribution. This is evidenced by thinner north central Tibetan crust overlying significantly slow asthenospheric mantle being at the same elevation as thicker southern Tibetan crust overlying thick CML (Owens and Zandt, 1997; Fig. 3).

If the properties of the crust—particularly its integrated strength—dictate the height and thickness of Tibet, then this raises the question as to when the system evolved to that state. Crustal rheological models of Beaumont et al. (2004) are consistent with a fairly rapid (<15 m.y.) transition to plateau-like topography. Stable isotope paleoaltimetry estimates are compatible with such a time scale, with central Tibet having achieved elevations of ≥4 km by ca. 25 Ma (Ingalls et al., 2020; Rowley and Currie, 2006; Ding et al., 2022).

CONCLUSIONS

Our primary conclusion is that large (>10%) variations in uppermost mantle (≤220 km) shear wave velocity anomalies beneath Tibetan Plateau crust are uncorrelated with overlying surface topography but instead correlate nearly perfectly with variations in crustal thickness. In addition, the underthrusting Indian CML has been migrating northward over the past 25 m.y., yet there is no evidence for any topographic response to this process. This strongly implies that Tibetan plateau crust is sufficiently weak that the crust is able to flow such that a relatively flat and high topography has been sustained over the past 25 m.y. as the Indian CML has progressively migrated northward. Borrowing an analogy from McKenzie et al. (2019), this is consistent with the Tibetan crust being equivalent to a reservoir of water with a thin layer of ice over geologic time.

ACKNOWLEDGMENTS

We acknowledge the Incorporated Research Institutions for Seismology Data Management Center (IRIS DMC); Japanese F-net Broadband Seismograph Network; China Earthquake Administration;

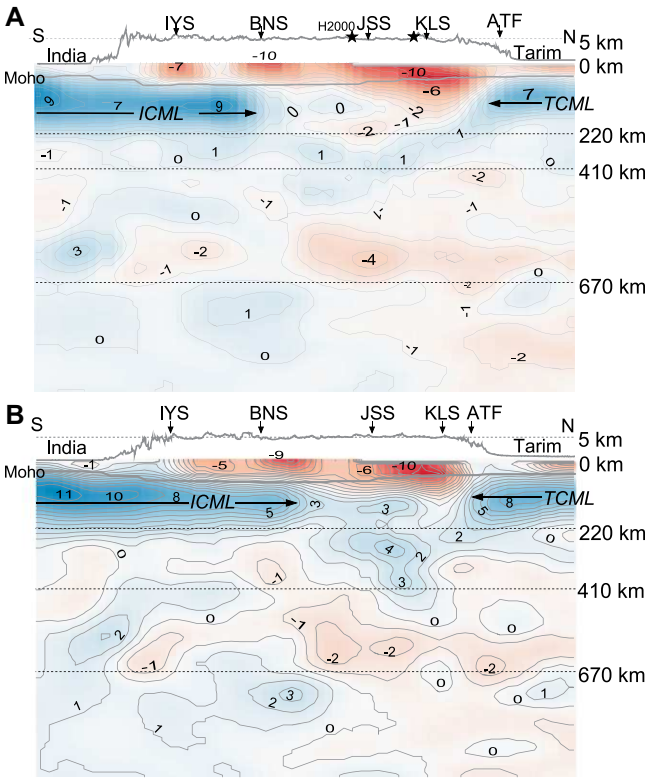

Figure 3. Cross sections from India to eastern Tarim Basin highlighting the lateral extent of underthrust Indian (ICML) and Tarim (TCLM) cratonic mantle lithosphere. Location of the sections is shown on Figure 2B. Upper boundary is vertically exaggerated (~×15) topography relative to the tomography. Contour interval is 1% in Vs at 100 km depth. Locations of 0 Ma to 5 Ma volcanism shown by stars, with projected location of Hacker et al. (2000) as H2000 on Figure 3A. Color scale same as Figure 2B. ATF—Altyn Tagh fault; BNS—Bangong Co-Nujiang suture; IYS—Indus-Yarlung suture; JSS—Jinsha suture; KLS—Kunlun suture.

Indian National Centre; National Center for Seismology (India); Deep Continental Studies (DST-DCS) program in Sikkim; Jammu and Kashmir Seismological Network (JAKSNET); Northeast China Extended Seismic Array (NECESSArray); the Thailand TM seismic network; Earth Observatory of Singapore (EOS) Myanmar seismic network; Bangladesh-India-Myanmar (BIMA) temporary networks; Thai Seismic Array (TSAR); and other regional seismic networks for providing seismic waveform data used in this study. Xiaofeng Liang is supported by NSFC (92355301, 42074067) and Key Research Program of IGGCAS (202204). We thank the Texas Advanced Computing Center at the University of Texas at Austin for high-performance computing resources. We thank Kai Tao for help with using SPECFEM3D_Globe code. We thank Simon Klemperer, Bernhard Steinburger, Paul Kapp, and two anonymous reviewers for their constructive comments.

REFERENCES CITED

Amante, C., and Eakins, B.W., 2009, ETOPO1 1 Arc-Minute Global Relief Model: Procedures, Data Sources, and Analysis: U.S. Department of Commerce, National Oceanic and Atmospheric Administration Technical Memorandum NESDIS NGDC-24, v. 24, 19 p.

Argand, E., 1924, La Tectonique de L'Asie, *in* Proceedings of the XIIIth International Geological Congress: Brussels, Belgium, 10–19 August 1922, v. 1, pt. 5, p. 181–372.

Beaumont, C., Jamieson, R.A., Nguyen, M.H., and Medvedev, S., 2004, Crustal channel flows: 1. Numerical models with applications to the tectonics of the Himalayan-Tibetan orogen: Journal of Geophysical Research: Solid Earth, v. 109, https://doi.org/10.1029/2003JB002809.

Chapman, J.B., and Kapp, P., 2017, Tibetan Magmatism Database: Geochemistry, Geophysics, Geosystems, v. 18, p. 4229–4234, https://doi.org/10.1002/2017GC007217.

Ding, L., Kapp, P., Cai, F., Garzione, C.N., Xiong, Z., Wang, H., and Wang, C., 2022, Timing and mechanisms of Tibetan Plateau uplift: Nature Reviews: Earth & Environment, v. 3, p. 652–667, https://doi.org/10.1038/s43017-022-00318-4.

Dou, H., Xu, Y., Lebedev, S., Chagas de Melo, B., van der Hilst, R.D., Wang, B., and Wang, W.A., 2024, The upper mantle beneath Asia from seismic tomography, with inferences for the mechanisms of tectonics, seismicity, and magmatism: Earth-Science Reviews, v. 255, https://doi.org/10.1016/j.earscirev.2024.104841.

England, P., and Houseman, G., 1986, Finite strain calculations of continental deformation. 2. Comparison with the India-Asia collision zone: Journal of Geophysical Research: Solid Earth and Planets, v. 91, p. 3664–3676, https://doi.org/10.1029/JB091iB03p03664.

England, P., and McKenzie, D., 1982, A thin viscous sheet model for continental deformation: Geophysical Journal of the Royal Astronomical Society, v. 79, p. 285–321.

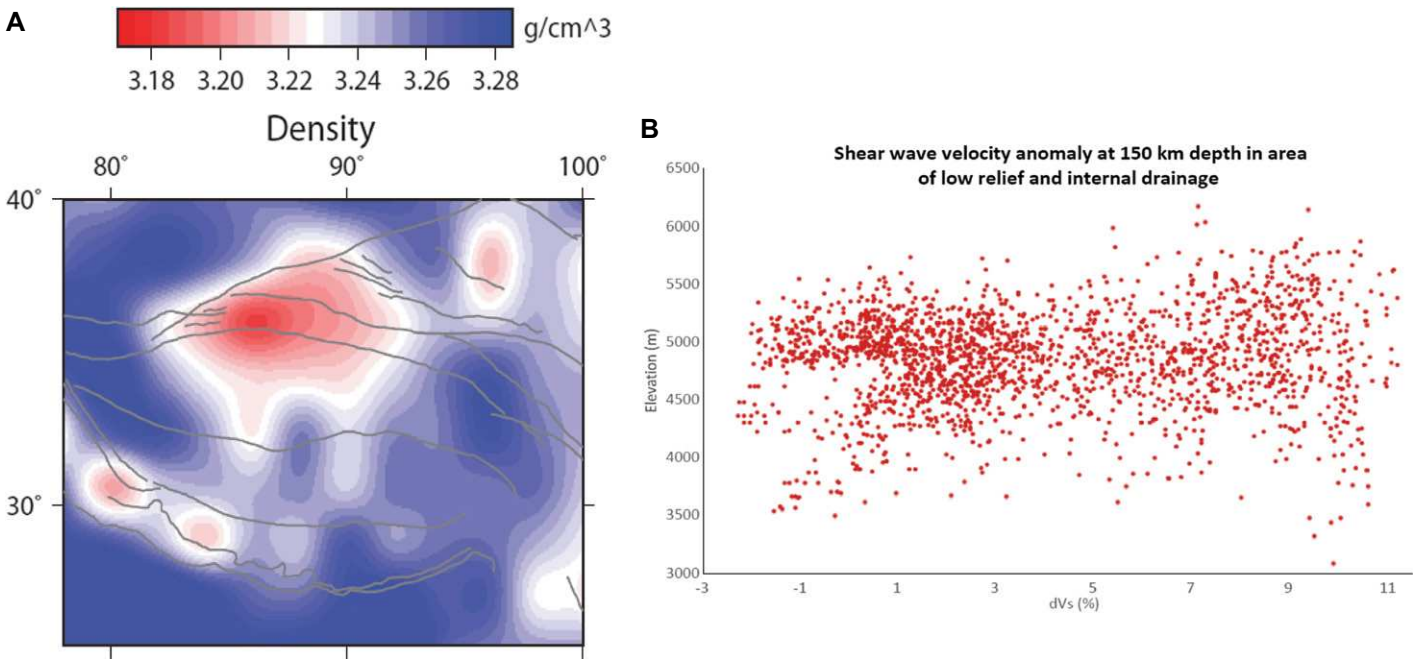

Figure 4. (A) Plot of the predicted density anomalies needed to maintain a 5 km topography using the crustal thickness model of Liang et al. (2023). (B) Correlation of elevation with upper mantle shear wave velocity anomaly at 150 km.

Hacker, B.R., Gnos, E., Ratschbacher, L., Grove, M., McWilliams, M., Sobolev, S.V., Wan, J., and Zhenhan, W., 2000, Hot and dry deep crustal xenoliths from Tibet: Science, v. 287, p. 2463–2466, https://doi.org/10.1126/science.287.5462.2463.

Hao, A., Zhang, H., Han, S., and Maceira, M., 2023, High-resolution lithospheric structure of continental China from joint inversion of surface wave and gravity data: Tectonophysics, v. 868, https://doi.org/10.1016/j.tecto.2023.230079.

Ingalls, M., Rowley, D.B., Currie, B.S., and Colman, A.S., 2020, Reconsidering the uplift history and peneplanation of the northern Lhasa terrane, Tibet: American Journal of Science, v. 320, p. 479–532, https://doi.org/10.2475/06.2020.01.

Liang, X., Chen, L., Tian, X., Chu, Y., and Li, W., 2023, Uplifting mechanism of the Tibetan Plateau inferred from the characteristics of crustal structures: Science China: Earth Sciences, v. 66, p. 2770–2790, https://doi.org/10.1007/s11430-023-1158-5.

Liu, C., Banerjee, R., Grand, S.P., Sandvol, E., Mitra, S., Liang, X., and Wei, S., 2024, A high-resolution seismic velocity model for East Asia using full-waveform tomography: Constraints on India-Asia collisional tectonics: Earth and Planetary Science Letters, v. 639, https://doi.org/10.1016/j.epsl.2024.118764.

Ma, J., Bunge, H., Thrastarson, S., Fichtner, A., van Herwaarden, D., Tian, Y., Chang, S., and Liu, T., 2022, Seismic full-waveform inversion of the crust-mantle structure beneath China and adjacent regions: Journal of Geophysical Research: Solid Earth, v. 127, https://doi.org/10.1029/2022JB024957.

McKenzie, D., McKenzie, J., and Fairhead, D., 2019, The mechanical structure of Tibet: Geophysical Journal International, v. 217, p. 950–969, https://doi.org/10.1093/gji/ggz052.

Molnar, P., England, P., and Martinod, J., 1993, Mantle dynamics, uplift of the Tibetan Plateau, and the Indian Monsoon: Reviews of Geophysics, v. 31, p. 357–396, https://doi.org/10.1029/93RG02030.

Owens, T., and Zandt, G., 1997, Implications of crustal property variations for models of Tibetan plateau evolution: Nature, v. 387, p. 37–43, https://doi.org/10.1038/387037a0.

Parsons, A.J., Hosseini, K., Palin, R.M., and Sigloch, K., 2020, Geological, geophysical and plate kinematic constraints for models of the India-Asia collision and the post-Triassic central Tethys oceans: Earth-Science Reviews, v. 208, https://doi.org/10.1016/j.earscirev.2020.103084.

Rowley, D.B., and Currie, B.S., 2006, Palaeo-altimetry of the late Eocene to Miocene Lunpola basin, central Tibet: Nature, v. 439, p. 677–681, https://doi.org/10.1038/nature04506.

Royden, L.H., 1997, Surface deformation and lower crustal flow in eastern Tibet: Science, v. 276, p. 788–790, https://doi.org/10.1126/science.276.5313.788.

Schaeffer, A.J., and Lebedev, S., 2013, Global shear speed structure of the upper mantle and transition zone: Geophysical Journal International, v. 194, p. 417–449, https://doi.org/10.1093/gji/ggt095.

Tao, K., Grand, S.P., and Niu, F., 2018, Seismic structure of the upper mantle beneath eastern Asia from full waveform seismic tomography: Geochemistry, Geophysics, Geosystems, v. 19, p. 2732–2763, https://doi.org/10.1029/2018GC007460.

Valdes, P.J., Lin, D., Farnsworth, A., Spicer, R.A., Li, S.-H., and Tao, S., 2019, Comment on "Revised paleoaltimetry data show low Tibetan Plateau elevation during the Eocene": Science, v. 365, https://doi.org/10.1126/science.aax8474.

Printed in the USA